EFFECTS OF DEPOSITION ENERGY ON MICROSTRUCTURE AND MAGNETIC PROPERTIES OF NANOCOMPOSITES

An Undergraduate Research Scholars Thesis

by

MATIAS KALASWAD

Submitted to the Undergraduate Research Scholars program at
Texas A&M University
in partial fulfillment of the requirements for the designation as an

UNDERGRADUATE RESEARCH SCHOLAR

Approved by Research Advisor: Dr. Haiyan Wang

May 2017

Major: Electrical Engineering

TABLE OF CONTENTS

ABSTRACT

Effects of Deposition Energy on Microstructure and Magnetic Properties of Nanocomposites

Matias Kalaswad
Department of Electrical Engineering
Texas A&M University

Research Advisor: Dr. Haiyan Wang
Department of Electrical Engineering
Texas A&M University

Recent studies have shown that vertically aligned nanocomposite (VAN) materials possess many unique properties, including ferromagnetism. These properties can be used for spintronic applications, such as high density data storage or magnetoresistive random-access memory. Vertical iron pillars within $La_{0.5}Sr_{0.5}FeO_3$ have been studied before, but work remains to optimize their growth for practical spintronic applications. In this study, $(La_{0.5}Sr_{0.5}FeO_3)_{0.94}$:$(Fe_2O_3)_{0.06}$ targets were created and deposited onto $SrTiO_3$ substrates by pulsed laser deposition. Laser energy was varied between 300 and 450 mJ. The results suggest that deposition energy plays an important role in the formation of microstructures, and by extension, their magnetic properties. This study explores the effects deposition energy has on microstructure and ferromagnetic properties in VAN thin films, thereby making more precise property-control possible. This introduces the potential for further studies, such as varying target stoichiometry or deposition frequency.

DEDICATION

For my grandparents, mother, father, and sister.

ACKNOWLEDGEMENTS

I would like to thank my mentor and future graduate advisor, Dr. Haiyan Wang, for her guidance and support throughout the course of this research. I would also like to thank Bruce Zhang, Leigang Li, and Meng Fan for teaching me how to use the lab equipment and helping me in various ways throughout my undergraduate research experience.

I also want to extend my gratitude to the U.S. National Science Foundation DMR-1401266 (Texas A&M University) and DMR-1643911 (Purdue University), which partially supported this research project. Bruce Zhang and Leigang Li acknowledge the support from the Office of Naval Research (N00014-15-1-2362 Texas A&M and N00014-16-1-2465 Purdue University).

Finally, thanks to my mother and father for their encouragement.

NOMENCLATURE

LSFO	Abbreviation for chemical compound $La_{0.5}Sr_{0.5}FeO_3$
STO	Abbreviation for chemical compound $SrTiO_3$
VAN	Vertically aligned nanocomposite
PLD	Pulsed laser deposition
XRD	X-ray diffraction
TEM	Transmission electron microscopy
PPMS	Physical property measurement system

CHAPTER I

INTRODUCTION

Thin films are typically nano or micrometer-sized layers of film on a substrate. They are able to serve multiple physical applications, including protection, insulation, and data storage. Traditionally, growth of thin films has been laterally, parallel to the substrate. Recent findings have shown that it is also possible for growth to occur vertically, perpendicular to the substrate, giving rise to the field of VANs. The advantages of VAN films include tunable vertical lattice strain and interface coupling [1]. Physical properties can be enhanced to exploit new applications. Ferromagnetism, for example, is a property of certain materials that exhibit spontaneous magnetization. An induced magnetic field can cause the domains to line up in the same orientation, resulting in an overall magnetization of the material.

Perpendicular ferromagnetic nanowires are topic of interest due to their potential use in several areas of nanotechnology. Their strong magnetization makes them good candidates for high-density data storage [2]. One such ferromagnetic nanowire occurs during the deposition of LSFO [2]. Fe nanowires, also called nanopillars, are formed within the LSFO matrix and grow perpendicular to the substrate. Similar endeavors with $(La_{0.7}Sr_{0.3}MnO_3)_{0.5}$:$(ZnO)_{0.5}$ have shown that the tunability of physical properties is associated with the vertical phase boundaries that change as a function of the deposition frequency [3].

The purpose of this study is to explore the morphology and the magnetic property dependencies on growth conditions in Fe pillars within LSFO, namely laser energy during deposition. LSFO

targets doped with Fe_2O_3 were deposited on STO (001) substrates by PLD at laser energies of 300, 400, and 450 mJ. After deposition, various analyses were completed for microstructure and ferromagnetic characterization. The thin film samples were analyzed using XRD to determine the chemical composition and general lattice structure. The microstructure of the samples was determined via TEM, using cross-sectional images. Magnetization data was obtained with a vibrating sample magnetometer (VSM) in the PPMS.

CHAPTER II

METHODS

Ceramic sintering

The LSFO target was prepared using a ceramic sintering process. The metal oxide powders were weighed according to proper molar ratios, mixed using a mortar and pestle, compressed in a mold, and sintered.

Pulsed laser deposition

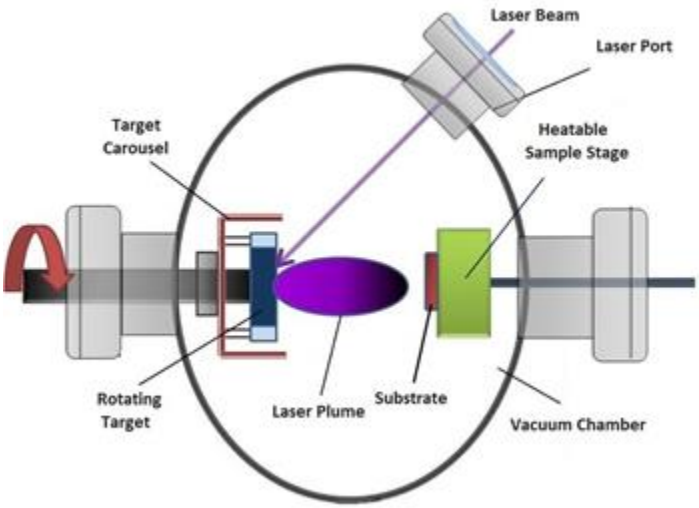

Figure 1. Pulsed laser deposition. Image source: groups.ist.utl.pt/rschwarz

Pulsed laser deposition (PLD) is a relatively simple deposition technique that offers the advantages of reproducing target stoichiometry with low contamination. PLD was utilized in this study to grow epitaxial thin films on single crystal substrates. During this process, a KrF excimer laser beam hits the target at near-vacuum pressure (<4E-6 mTorr) and generates a plume containing plasma, which deposits the compounds as thin films onto the substrate at high temperatures. Figure 1 illustrates this process.

X-ray diffraction

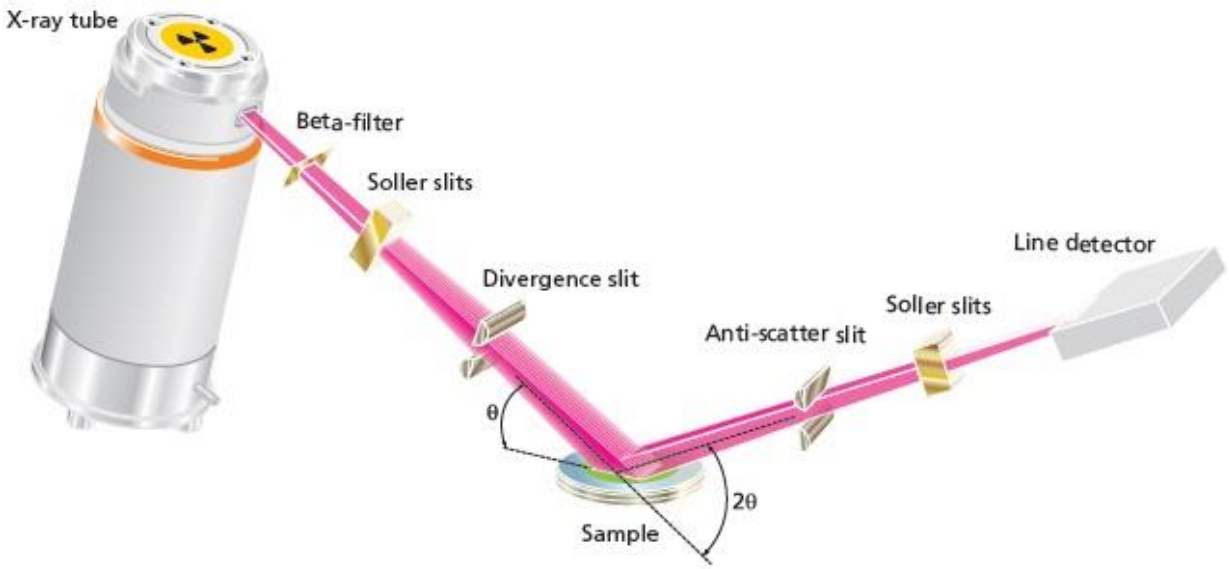

Figure 2. X-ray diffraction. Image source: usedscreeners.com

X-ray diffraction (XRD) was used to characterize the crystalline composition and structure of the samples. X-rays are produced by blasting a metal target with a beam of electrons emitted from a tungsten filament. When the X-rays interact with the sample, they scatter and undergo constructive and destructive interference in a process known as diffraction. Figure 2 illustrates this process. Using Bragg's Law, size and shape of the unit cells can be determined. A graphical plot of the intensity of the diffracted X-rays and the incident angle is generated. Crystalline structure can be found by comparing peaks on the diagram to a library of known compounds.

Transmission electron microscopy

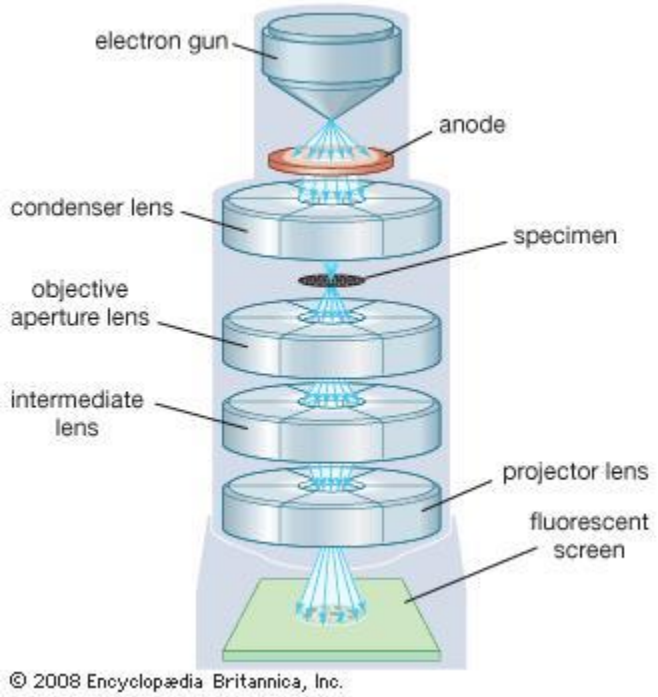

Figure 3. Transmission electron microscopy. Image source: britannica.com

Transmission electron microscopy (TEM) was used to assess film quality and determine the microstructure of the thin film samples. TEM takes advantage of the smaller wavelengths of electrons to achieve image resolution on the scale of nanometers. As shown in Figure 3, the electron microscope emits a high-energy beam of electrons, which passes through and interacts with an extremely thin sample. The transmitted electron beam magnifies and focuses on the image, which displays the atomic structure on a screen.

Physical property measurement system

Figure 4. Physical property measurement system. Image source: ahxinan.com

A physical property measurement system (PPMS), in conjunction with a vibrating system module (VSM), was used to determine the magnetic response of the thin film samples in response to an applied magnetic field. This system is also capable of measuring resistivity, AC transport, and Hall Effect.

Experimental procedure

A composite target ($La_{0.5}Sr_{0.5}FeO_3$: Fe_2O_3 94:6 molar ratio) was prepared using conventional ceramic sintering processes. The epitaxial film was grown on STO (001) substrates at 750ºC under a high vacuum (<4E-6 mTorr) via PLD using a KrF excimer laser (λ = 248 nm) with a laser fluence of 1.9 J/cm^2 and a frequency of 5 Hz to grow a target film thickness range of 80-100 nm. After deposition, the films immediately cooled to 20ºC under a vacuum.

The film's epitaxial quality was characterized by XRD (Panalytical X'Pert X-ray Diffractometer), its microstructure was studied via TEM (FEI Technai G2 F20), and magnetic measurements were done at 300 K using a PPMS (Quantum Design), specifically with the VSM with an applied magnetic field of -5000 to 5000 T.

CHAPTER III

RESULTS

X-ray diffraction

XRD was used to verify the quality of growth in the LSFO:Fe_2O_3 film. The epitaxial growth of the 300 mJ, 400 mJ, and 450 mJ samples is verified from the θ-2θ XRD scans in Figure 5. Centered around the STO (002) peak are distinct Fe (110), $LaSrFeO_4$ (006), and $La_{0.5}Sr_{0.5}FeO_3$ (200) peaks that confirm the decomposition of $La_{0.5}Sr_{0.5}FeO_3$ (200) [2]. In the 300 mJ and 450 mJ samples, the Fe (110) peak rests around a 2θ of 45 degrees, while for the 400 mJ sample, the Fe (110) peak rests around a 2θ of 44.6 degrees. The Fe (110) peak of the 400 mJ sample is shifted further left from the STO (200) peak compared to the 300 mJ and the 400 mJ (Figure 6), resulting in the Fe (110) being more strained within the 400 mJ sample.

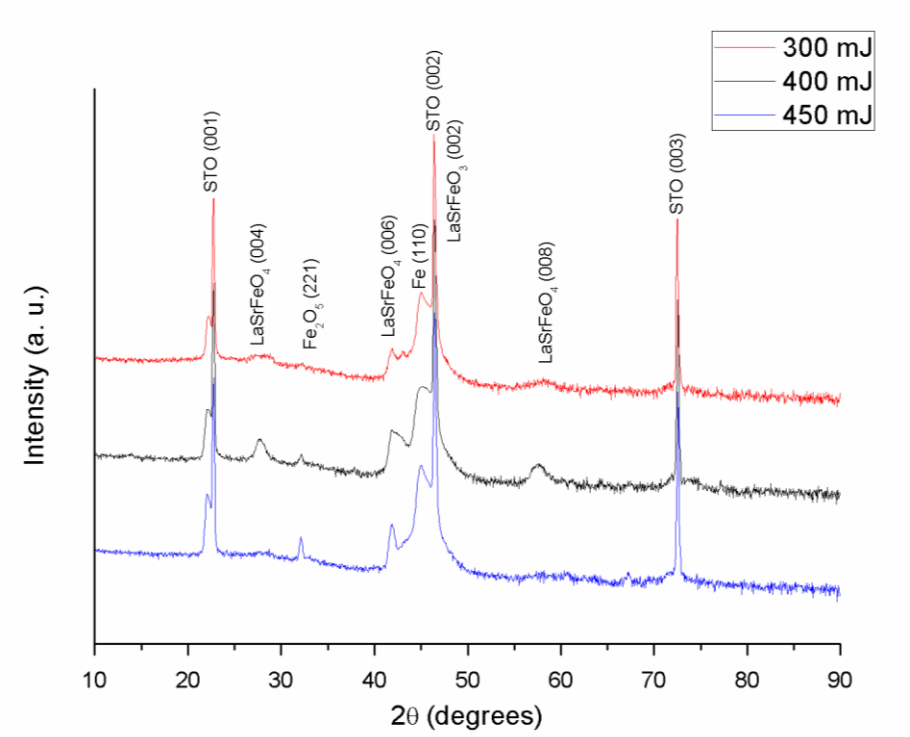

Figure 5. XRD plot comparing samples grown at various energies

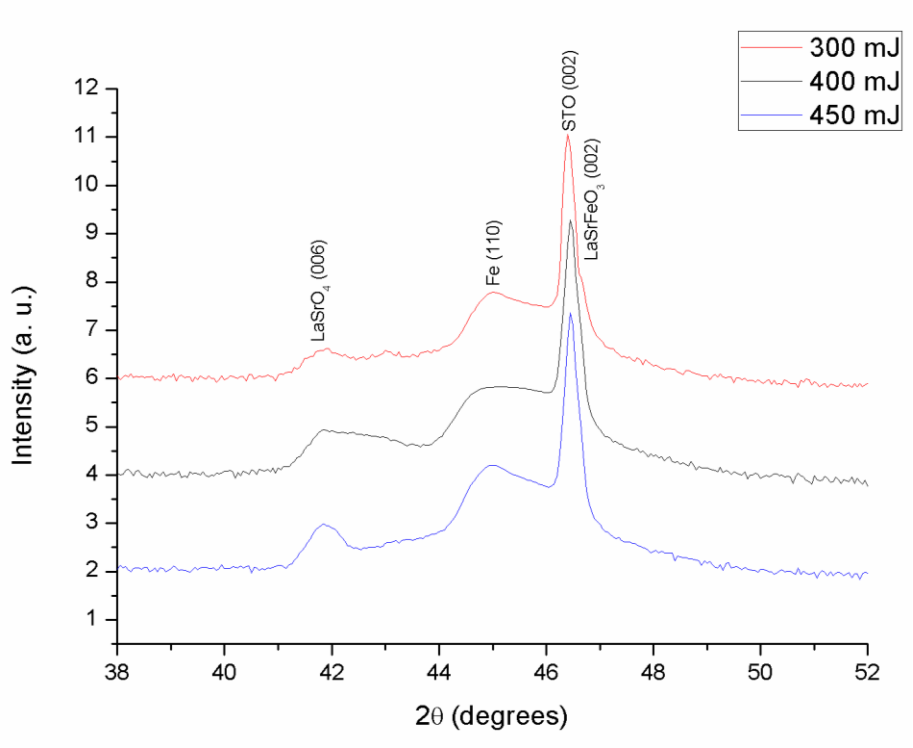

Figure 6. XRD plot magnified to show shift of Fe (110) peaks

Transmission electron microscopy

To assess the film quality and determine the microstructure of the samples, cross-sectional and plan-view TEM study was prepared and studied. The thickness of all three films is approximately 100 nm.

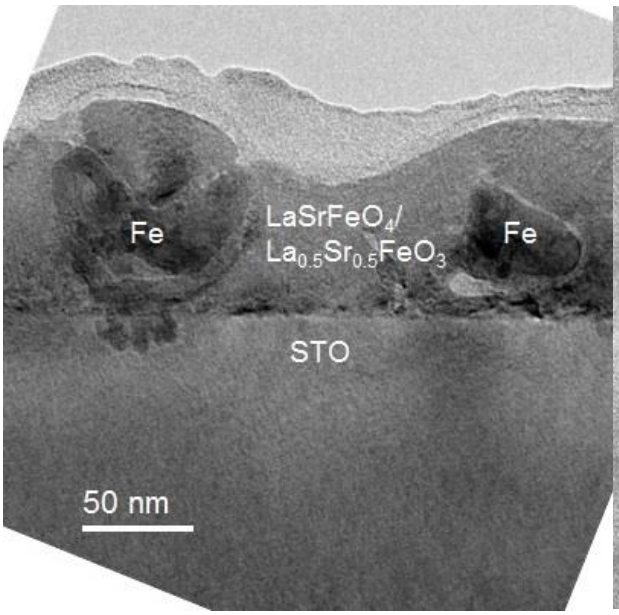

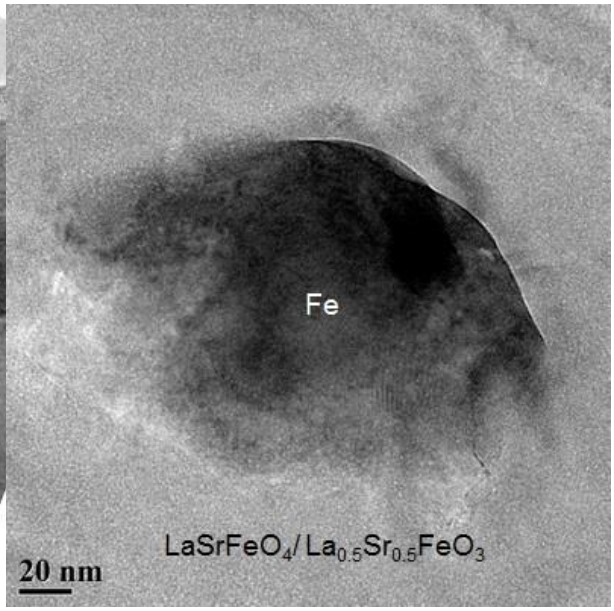

Figure 7. TEM cross-section of 300 mJ

Figure 8. TEM plan-view of 300 mJ

Cross-sectional images were obtained for regions on the film grown at laser energy 300 mJ. Figure 7 shows two distinct clumps that are characteristic of particle growth. Plan-view analysis of this sample, seen in Figure 8, reveals large circular Fe particles. These observations suggest that particle growth is representative of $(La_{0.5}Sr_{0.5}FeO_3)_{0.94}$:$(Fe_2O_3)_{0.06}$ grown at 300 mJ.

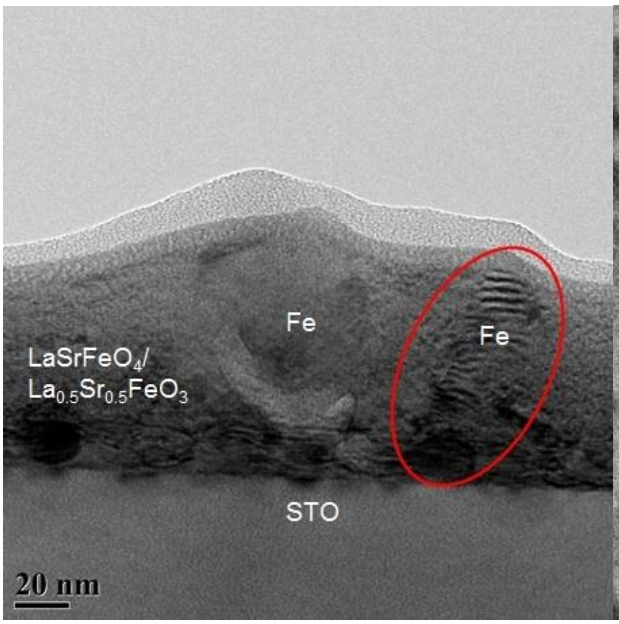

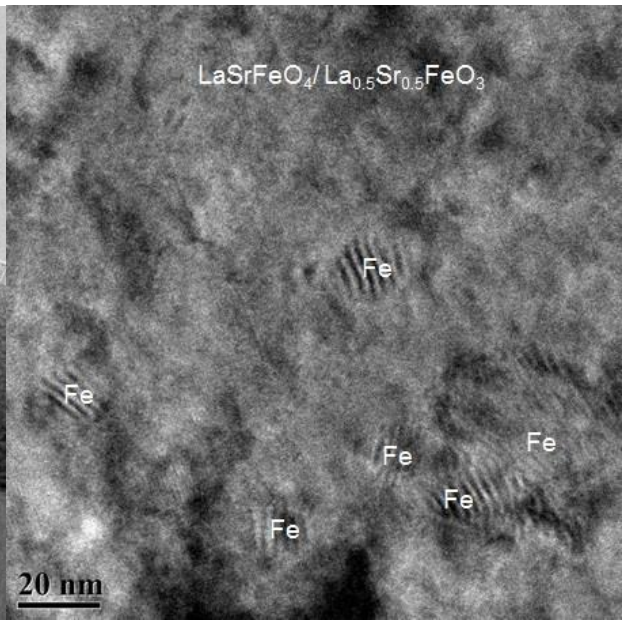

Figure 9. TEM cross-section of 400 mJ

Figure 10. TEM plan-view of 400 mJ

Cross-sectional TEM images were also achieved for three regions on the film grown at 400 mJ. In the 400 mJ sample, Figure 9 shows clumps that resemble particle growth. However, upon closer inspection, pillar structures are clearly visible within the apparent clump. These pillars show clear epitaxial arrangement. Plan-view analysis of the 400 mJ sample, shown in Figure 10, is a confirmation of the cross-section image. The same type of organized growth is seen in this image. This data seems to propose that epitaxial pillar-like growth is predominant in the 400 mJ thin film sample.

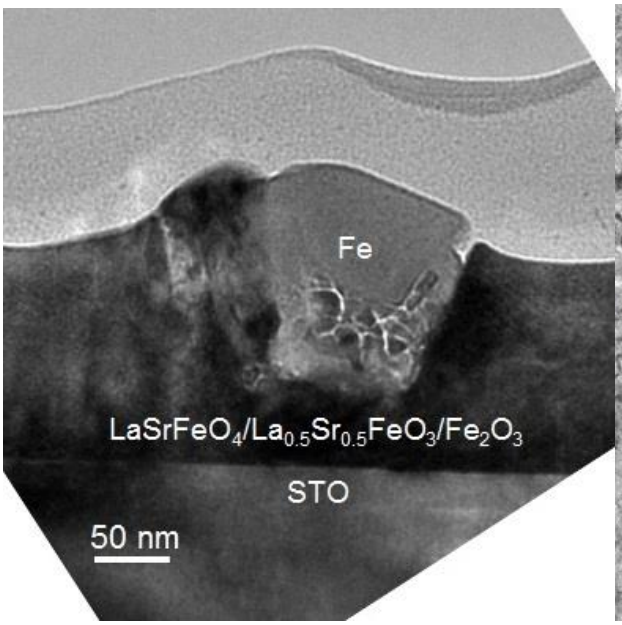

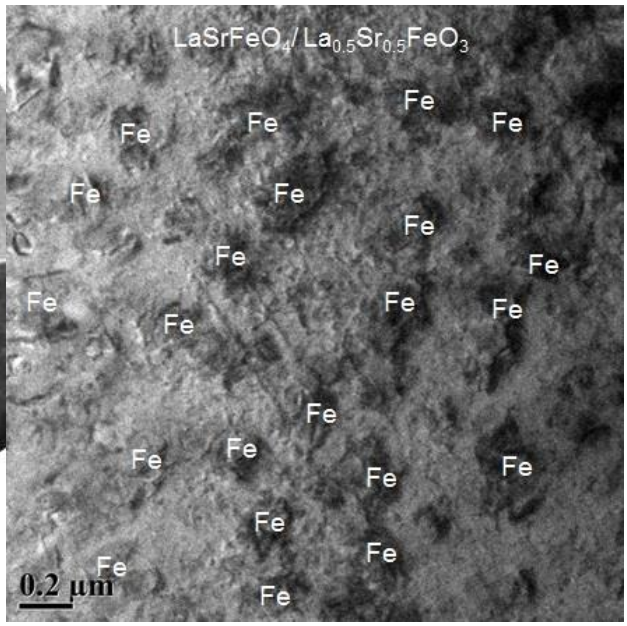

Figure 11. TEM cross-section of 450 mJ

Figure 12. TEM plan-view of 450 mJ

The 450 mJ sample consists primarily of particle growth consisting of Fe clusters, as seen in Figure 11. This sample lacks the ordered arrangement that is typical of epitaxial, pillar growth. Plan-view analysis of this sample, seen in Figure 12, also indicates an abundance of particle growth. The dark spots are indicative of Fe growth, which do not contain any visible pillars. These observations suggest that particle growth is representative of $(La_{0.5}Sr_{0.5}FeO_3)_{0.94}$:$(Fe_2O_3)_{0.06}$ grown at 450 mJ.

Physical property measurement system

To demonstrate the magnetic applications of these metal VANs, their magnetic properties were measured in both the in-plane and out-of-plane directions. The in-plane magnetic hysteresis loop is shown in Figure 13 and the out-of-plane loop is shown in Figure 14. The samples grown at 300 and 400 mJ have magnetic moments that are anisotropic, with the out-of-plane magnetic moment being significantly larger than the in-plane. On the other hand, the 450 mJ sample shows isotropic properties.

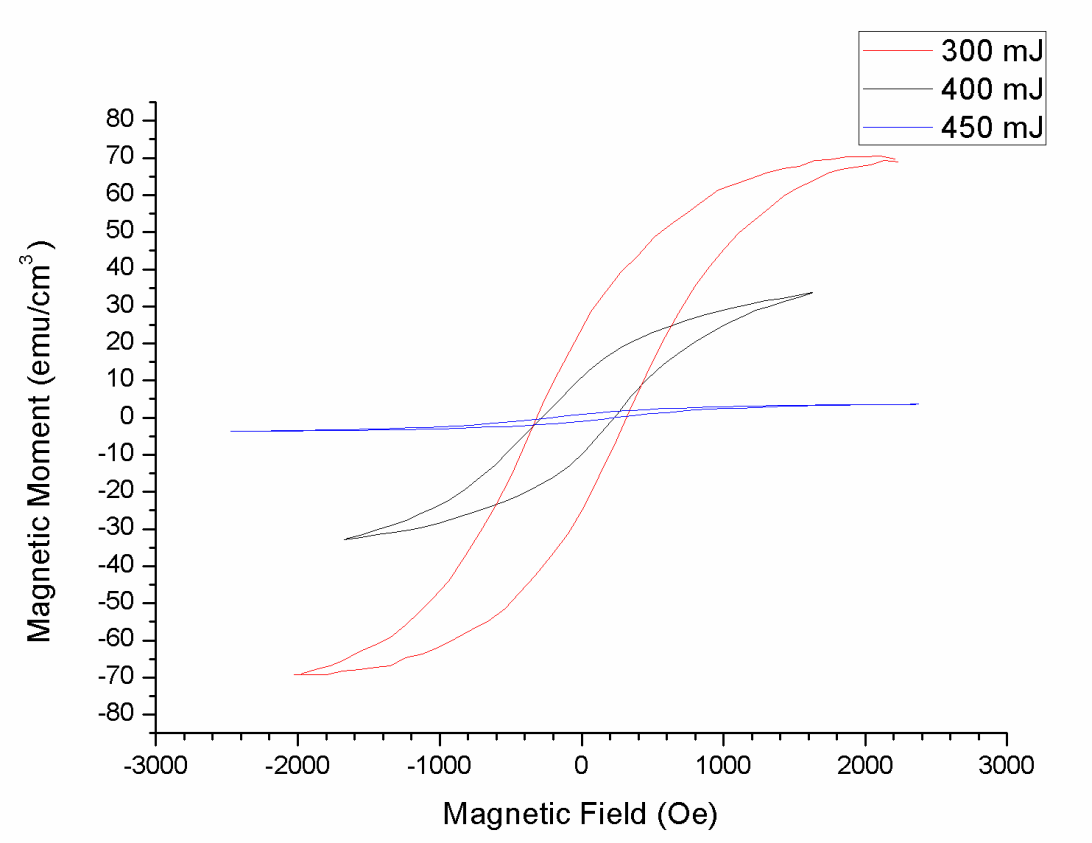

Figure 13. In-plane magnetic response to an applied magnetic field

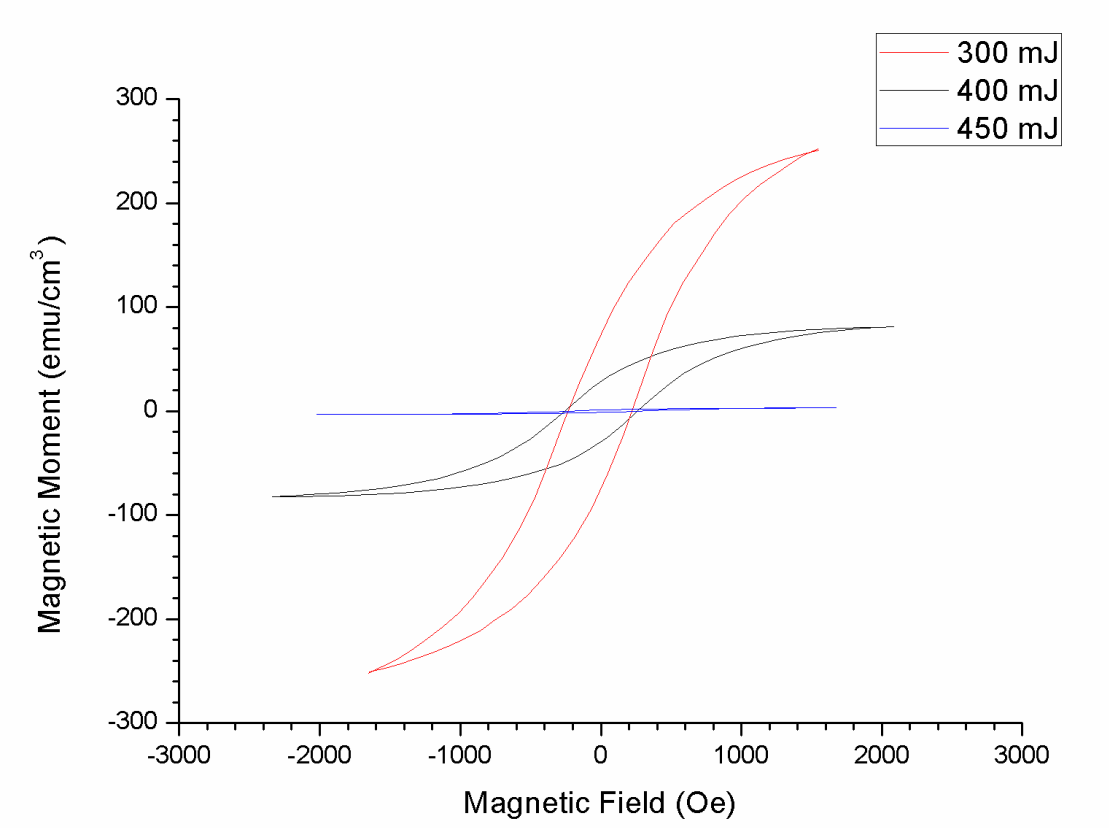

Figure 14. Out-of-plane magnetic response to an applied magnetic field

Furthermore, the out-of-plane and in-plane magnetic moment at an applied magnetic field of 1500 T is shown to increase with decreasing deposition energy, as seen in Figure 15. This response can be attributed to the Fe microstructure and size. The microstructure of the Fe in the 450 mJ sample contains particles with similar vertical and horizontal size, resulting in an isotropic magnetic moment. In contrast, the microstructure of the Fe in the 400 mJ sample has epitaxial column growth. The diameter of the pillars is around 10 nm while the height goes through the entire film, resulting in a stronger vertical magnetic direction compared to the horizontal magnetic direction due to the increased amount of Fe. The microstructure of the Fe in the 300 mJ sample follows the same pattern as the 400 mJ sample, but the diameter of the Fe particle is around 50 nm. The larger size suggests more Fe exists in both the vertical and horizontal directions, resulting in a larger magnetic moment.

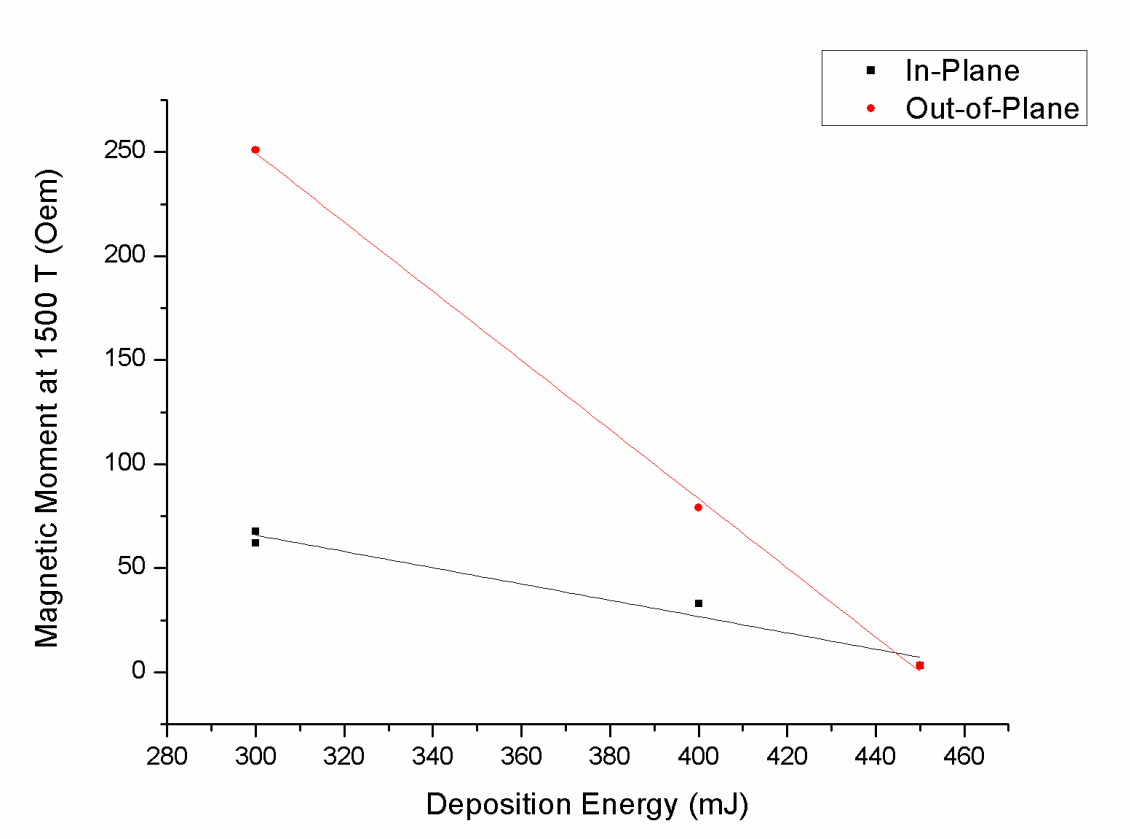

Figure 15. Relationship between magnetic moment at 1500 T and deposition energy

CHAPTER IV

CONCLUSION

Previous studies have shown that in other films, such as Cu_2ZnSnS_4 and FeF_2, deposition energy plays a role in film morphology and microstructure [4,5]. The results of this study suggest that at 300 mJ, the Fe atoms do not have sufficient kinetic energy to travel long enough distances to organize themselves into uniform, epitaxial layers [6]. In this state, they are unable to form ordered pillar structures which results in a larger 50 nm microstructure size. At higher deposition energies, such as 450 mJ, the Fe atoms can overcome the binding energy of the neighboring particles, resulting in the Fe atoms to be able to go into the more relaxed, energy favorable, particle microstructure. In the thin film grown at 400 mJ, the Fe atoms have sufficient energy to grow into epitaxial ordered column growth, but not enough to overcome the binding energy, resulting a more strained pillar growth.

Growth by PLD and analytical methods including XRD and TEM were used to confirm that deposition laser energy plays a critical role in both the microstructure and ferromagnetic response of LSFO thin films. The approach of varying laser energy during deposition was effective, with the observations indicating that optimal microstructure, pillar, growth occurs around a laser energy of 400 mJ. Similarly, optimum ferromagnetic response was observed at 300 mJ. These results are beneficial to the field of spintronics, where significant work remains to optimize their growth for practical applications. This is an area that warrants future exploration. By improving film quality, applications such as high density data recording and multifunctional devices can be achieved.

REFERENCES

[1] W. Zhang, “Enchanced functionalities achieved by a vertically aligned nanocomposite approach,” Ph.D. dissertation, Dept. Elect. Eng., Texas A&M Univ., College Station, TX, 2015.

[2] L. Mohaddes-Ardabili, H. Zheng, S.B. Ogale, B. Hannoyer, W. Tian, J. Wang, S.E. Lofland, S.R. Shinde, T. Zhao, Y. Jia, L. Salamanca-Riba, D.G. Schlom, M. Wuttig, R. Ramesh, Self-assembled single-crystal ferromagnetic iron nanowires formed by decomposition, Nat. Mater., 3 (2004), pp. 533–538

[3] A. Chen, Z. Bi, Chen-Fong Tsai, J. H. Lee, Q. Su, X. Zhang, Q. X. Jia, J. L. MacManus-Driscoll and H. Wang. Tunable Low-Field Magnetoresistance in $(La_{0.7}Sr_{0.3}MnO_3)_{0.5}$:$(ZnO)_{0.5}$ Self-Assembled Vertically Aligned Nanocomposite Thin Films, Advanced Functional Materials, 21, 2423, (2011).

[4] Pawar, S. M., Moholkar, A. V, Kim, I. K., Shin, S. W., Moon, J. H., Rhee, J. I., & Kim, J. H. , Effect of laser incident energy on the structural , morphological and optical properties of Cu 2 ZnSnS 4 (CZTS) thin films. Current Applied Physics, 10, 565–569 (2010).

[5] Jitendra, R. S., Jha, K., & Rojhirunsakool, T. Effect of deposition energy on the microstructure and phase purity of pulsed laser deposited iron fluoride thin films. Applied Physics A, 120, 863–868(2015).

[6] Muller, K. Role of Incident Kinetic Energy of Adatoms in Thin Film Growth. Surface Science Letters, 184, 375-382 (1987).